

# CALCULATION OF THE SPALDING FUNCTION OVER A RANGE OF PRANDTL NUMBERS

G. O. GARDNER\* and J. KESTIN†

(Received 11 September 1962)

**Abstract**—The paper presents an extensive tabulation of the Spalding function  $Sp = St \cdot Pr / (\frac{1}{2}c_f)^{1/2}$  which is very useful in the calculation of heat transfer rates into fully developed turbulent boundary layers. Numerical data are presented for  $Pr = 0.71, 1, 7, 30, 100$  and  $1000$ .

## NOMENCLATURE

$a$ ,	thermal diffusivity;	$\psi$ ,	stream function;
$a_e$ ,	effective thermal diffusivity;	$\varphi$ ,	stability criterion for numerical scheme;
$a_t$ ,	eddy, or turbulent thermal diffusivity;	$\tau$ ,	shearing stress;
$c_f$ ,	skin-friction coefficient;	$\tau_w$ ,	shearing stress at the wall;
$c_p$ ,	specific heat at constant pressure;	$\mu$ ,	absolute viscosity;
$k$ ,	thermal conductivity;	$\mu_e$ ,	effective viscosity;
$k_t$ ,	turbulent, or eddy thermal conductivity;	$\mu_t$ ,	eddy viscosity (absolute);
$Pr$ ,	Prandtl number;	$\nu$ ,	kinematic viscosity;
$Pr_e$ ,	effective Prandtl number;	$\nu_e$ ,	effective kinematic viscosity;
$Pr_t$ ,	turbulent Prandtl number;	$\nu_t$ ,	eddy viscosity (kinematic);
$\dot{q}$ ,	heat flux;	$\xi$ ,	reduced independent variable, equation (24);
$Re_x$ ,	Reynolds number based on length;	$\eta$ ,	similarity variable, equation (27a).
$Sp$ ,	Spalding function, equation (26);		
$St$ ,	Stanton number;		
$T$ ,	temperature;		
$T_w$ ,	temperature at wall;		
$T_\infty$ ,	temperature in free stream;		
$u$ ,	longitudinal velocity component;		
$u^+$ ,	reduced velocity, equation (8a);		
$U_\infty$ ,	free-stream velocity;		
$v$ ,	transverse velocity;		
$v_*$ ,	friction velocity, equation (8b);		
$x$ ,	length co-ordinate;		
$x^+$ ,	reduced length co-ordinate, equation (16);		
$y$ ,	transverse co-ordinate;		
$y^+$ ,	reduced transverse co-ordinate, equation (8).		

## Greek symbols

$\rho$ ,	density;
$\theta$ ,	reduced temperature, equation (2);

\* Graduate Student in Applied Mathematics at Brown University.

† Professor of Engineering at Brown University.

## 1. EXPOSITORY REMARKS

IN A PREVIOUS paper, Kestin and Persen [1] computed the so-called Spalding function for a Prandtl number equal to unity. Smith and Shah [2] adapted the underlying method to the calculation of Spalding functions to specified flux conditions at the wall, rather than to constant temperature conditions stipulated in [1]. Both papers were a development of an idea first suggested by Spalding [3] for the solution of the problem of the thermal entry length in a fully developed turbulent boundary layer.

In order to acquaint the reader with the ramifications of the calculations presented in the succeeding sections of this paper, it seems advisable briefly to outline the theory and the class of problems to which it can be applied.

The theory initiated by Spalding [3] and later discussed by Kestin and Richardson [4, 5], aims at providing a rational basis for the calculation of heat transfer into two-dimensional, incompressible, turbulent boundary layers. It is hoped

that further refinements of the theory will result in the establishment of a generally valid, semi-empirical differential equation for the calculation of turbulent forced convection. At present, the theory is restricted to flows for which the thermodynamic properties of the fluid can be assumed independent of temperature.

It is assumed by way of working hypothesis that the local mean energy balance in a turbulent boundary layer is governed by an equation identical with that in laminar flow:

$$\rho c_p \left( u \frac{\partial \theta}{\partial x} + v \frac{\partial \theta}{\partial y} \right) = \frac{\partial \dot{q}}{\partial y}, \quad (1)$$

except for two circumstances. The local velocity components  $u$ ,  $v$  and the local normalized temperature

$$\theta = \frac{T_\infty - T}{T_\infty - T_w} \quad (2)$$

( $T_\infty$ —uniform temperature at infinity;  $T_w$ —temperature at the wall) have been averaged with respect to time, and are thus steady. The local heat flux  $\dot{q}$  is composed of two terms, both proportional to the local temperature gradient  $\partial\theta/\partial y$ , one due to pure molecular conduction, the other due to turbulent exchange. Hence

$$\dot{q} = (k + k_t) \frac{\partial \theta}{\partial y}, \quad (3)$$

where  $k$  is the molecular thermal conductivity and  $k_t$ † is its “eddy” analogue. In this manner the familiar form of the energy equation is obtained:

$$u \frac{\partial \theta}{\partial x} + v \frac{\partial \theta}{\partial y} = \frac{\partial}{\partial y} \left( a_e \frac{\partial \theta}{\partial y} \right), \quad (4)$$

where

$$a_e = a + a_t \quad (5)$$

is the “effective” thermal diffusivity.

The unavoidable empirical statement regarding the function  $a_t(x, y)$  is obtained by considering the ratio

$$Pr_t = \frac{\nu_t}{a_t} \quad (6)$$

† We prefer to denote the eddy coefficients by the same symbols as those used for their molecular analogues, appending the subscript  $t$  for distinction. The resulting formulae are somewhat more symmetrical and easier to memorize.

of the eddy kinematic viscosity to eddy diffusivity, and by provisionally assuming, with Reynolds [6], that

$$Pr_t = 1, \quad (7)$$

provisionally, that is, until more is learned about it. The empirical formulation of the function  $\nu_t(x, y)$  is replaced by the adoption of the validity of a universal law of the wall [7, 8, 9] in the form

$$u^+ = \varphi(y^+) \quad (8)$$

where

$$u^+ = \frac{u}{v_*}, \quad y^+ = \frac{y v_*}{\nu} \quad (8a)$$

and

$$v_* = \left( \frac{\tau_w}{\rho} \right)^{1/2} \quad (8b)$$

is the friction velocity.

In heat transfer problems it is only necessary to ensure that the form of the law of the wall (8) is adequate over a distance from the wall roughly equal to that over which the thermal profile changes rapidly. Thus the “law of the wake” [8] can be disregarded, at least provisionally and certainly for high Prandtl numbers.

The particular form of (8) is of secondary importance, as long as it conforms to experimental results. It is preferable to use a single, continuous relation valid from the laminar sub-layer outwards, and for practical reasons, Spalding's [10] inverted law of the wall

$$y^+ = u^+ + 0.1108 \left[ e^{0.4u^+} - 1 - 0.4u^+ - \frac{1}{2}(0.4u^+)^2 - \frac{1}{6}(0.4u^+)^3 - \frac{1}{24}(0.4u^+)^4 \right] \quad (9)$$

proves to be most convenient.

Noting that the stream function

$$\psi = \int_0^y u \, dy$$

can be represented as

$$\psi = \nu \int_0^{y^+} u^+ \, dy^+ = \nu \int_0^{u^+} u^+ \left( \frac{dy^+}{du^+} \right) du^+, \quad (10)$$

it becomes apparent that replacing first  $y$  by  $\psi$  and then by  $u^+$  will lead to a considerable simplification of (4), since  $y^+$ ,  $\psi/\nu$  and  $u^+$  are unique functions of each other. Thus, Spalding applied the von Mises transformation to (4), and obtained

$$\frac{\partial \theta}{\partial x} = \frac{\partial}{\partial \psi} \left( a_e u \frac{\partial \theta}{\partial \psi} \right). \quad (11)$$

Replacing  $u$  by  $u^+$  and  $d\psi$  by  $\nu u^+(dy^+/du^+) du^+$ , at  $x = \text{const.}$ , from (10), we obtain

$$\frac{\nu}{v_*} \frac{\partial \theta}{\partial x} = \frac{1}{u^+} \frac{du^+}{dy^+} \frac{\partial}{\partial u^+} \left( \frac{a_e du^+}{\nu} \frac{\partial \theta}{\partial u^+} \right). \quad (12)$$

The eddy diffusivity, or its equivalent, the ratio  $a_t = \nu_t/Pr_t$  is now computed from the definition

$$\frac{\tau}{\tau_w} = \frac{\mu_e(\partial u/\partial y)}{\rho v_*^2} = \frac{\mu + \mu_t}{\mu} \frac{du^+}{dy^+}. \quad (13)$$

Hence  $a_e = \nu_e/Pr_e$  where

$$Pr_e = \frac{1 + \mu_t/\mu}{1/Pr + \mu_t/\mu \cdot 1/Pr_t} \quad (14)$$

and

$$\frac{\mu_e}{\mu} = 1 + \frac{\mu_t}{\mu} = \frac{\tau}{\tau_w} \cdot \frac{dy^+}{du^+}. \quad (15)$$

Introducing, finally, a new independent variable  $x^+$  to replace  $x$  by the definition

$$x^+ = \int_0^x \frac{v_* dx}{\nu}, \quad \left( \frac{dx^+}{dx} = \frac{v_*}{\nu} \text{ at } y = \text{const.} \right), \quad (16)$$

we can transform (11) to the *working equation*

$$\frac{\partial \theta}{\partial x^+} = \frac{1}{u^+} \frac{du^+}{dy^+} \frac{\partial}{\partial u^+} \left( \frac{1}{Pr_e} \frac{\tau}{\tau_w} \frac{\partial \theta}{\partial u^+} \right). \quad (17)$$

### 2. THE WORKING EQUATION

The working equation has one flaw, it contains the ratio  $\tau/\tau_w$  which must be computed from our knowledge of the flow field. However, it is known from elementary theories of turbulent convection [11] that the effect of this ratio on the final computation is not large. Secondly, as seen from Fig. 1, this ratio remains equal to unity for a considerable range of values of the

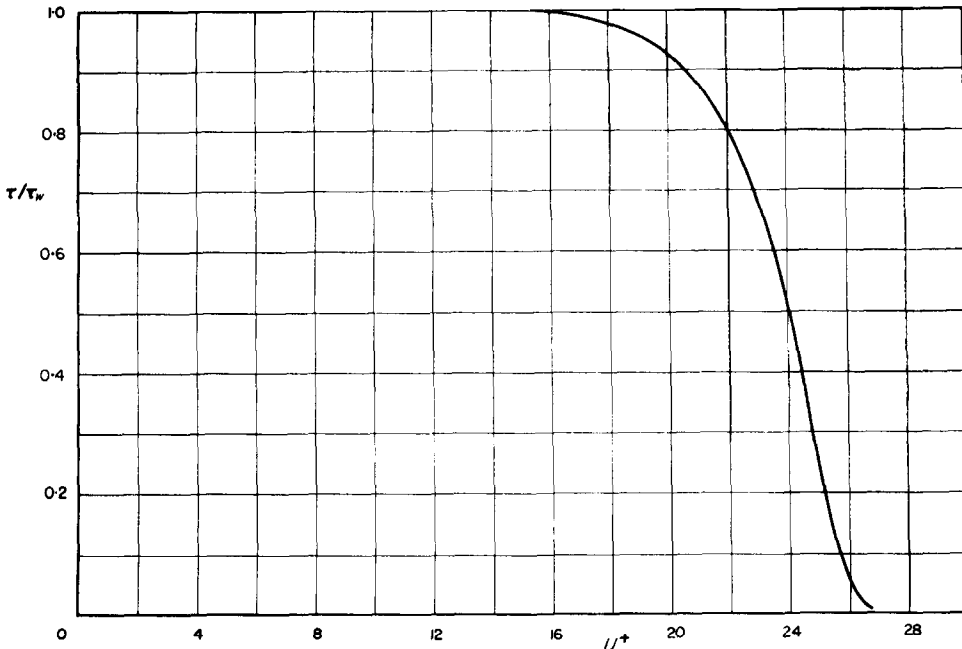


FIG. 1. Variation of ratio  $\tau/\tau_w$  across boundary layer on a flat plate. Measurements due to Klebanoff [12].

integration variable  $u^+$ . The diagram in Fig. 1 was computed from Klebanoff's [12] very careful measurements on a flat plate at  $Re_x = 4.2 \times 10^6$ . Thirdly, when the Prandtl number is large, or at the beginning of a thermal entry length, the thermal boundary layer is much smaller than the velocity boundary layer, and develops over a distance, that is over a range of values of  $u^+$ , over which  $\tau/\tau_w \sim 1$ , substantially.

Thus, as a first approximation, we put  $\tau/\tau_w = 1$ , and the working equation simplifies to

$$\frac{\partial \theta}{\partial x^+} = \frac{1}{u^+} \frac{du^+}{dy^+} \frac{\partial}{\partial u^+} \left( \frac{1}{Pr_e} \frac{\partial \theta}{\partial u^+} \right). \quad (18)$$

The simplified form lends itself to numerical integration in terms of  $u^+$  and  $x^+$ . The factors which translate  $x^+$  into  $x$  and  $u^+$  into  $y$  depend on the properties of the flow field which must be known in each particular case.

Noting that (18), or (17) for that matter, is linear and homogeneous, it is realized that solutions can be superimposed, and that it is sufficient to integrate (18) for one set of boundary conditions in order to obtain *universal functions* for the solution of problems in turbulent convection. The set of boundary conditions chosen is that of a thermal entry length.

$$\left. \begin{aligned} \theta &= 0 & \text{at } x^+ &= 0 & \text{and all } u^+ &> 0 \\ \theta &= 0 & \text{at } u^+ &= \infty & \text{and all } x^+ &> 0 \\ \theta &= 1 & \text{at } u^+ &= 0 & \text{and all } x^+ &> 0. \end{aligned} \right\} \quad (19)$$

For the calculation of heat transfer we need to know the so-called Spalding function

$$Sp(x^+, Pr) = - \left( \frac{\partial \theta}{\partial u^+} \right)_{u^+=0}. \quad (20)$$

The Spalding function contains the Prandtl number as a parameter in view of the relation in (14).

It is a simple matter to show that the local Stanton number,  $St$ , is related to the Spalding function,  $Sp$ , by the equation

$$St = Sp \cdot \frac{(\frac{1}{2}c_f)^{1/2}}{Pr}, \quad (21)$$

where

$$\frac{1}{2}c_f = \frac{\tau_w}{\rho U_\infty^2} = \left( \frac{v_*^*}{U_\infty} \right)^2. \quad (21a)$$

### 3. CALCULATION FOR $Pr = 1$

The calculations, performed by Schmidt's [13] step-by-step procedure on the Brown University IBM 7070 digital computer have been described elsewhere [1]. They related to the very simple equation

$$\frac{\partial \theta}{\partial x^+} = \frac{1}{f(u^+)} \frac{\partial^2 \theta}{\partial (u^+)^2}, \quad (22)$$

subject to the boundary conditions (19) with

$$\begin{aligned} f(u^+) &= u^+ + 0.04432u^+ \\ &\times \left[ e^{0.4u^+} - 1 - 0.4u^+ - \frac{1}{2}(0.4u^+)^2 \right. \\ &\quad \left. - \frac{1}{6}(0.4u^+)^3 \right]. \end{aligned} \quad (22a)$$

### 4. CALCULATION FOR $Pr \neq 1$

When the Prandtl number differs from unity, it is convenient to change to a new integration variable

$$\xi = \int_0^{u^+} Pr_e du^+. \quad (23)$$

Introducing the simplifying assumption that  $Pr_t = 1$  and the expression from (15) with the second simplifying assumption that  $\tau/\tau_w = 1$  into (14), we obtain

$$\xi = \int_0^{u^+} \frac{du^+}{dy^+} (1/Pr - 1) + 1, \quad (24)$$

and (17) transforms to

$$\frac{\partial \theta}{\partial x^+} = \frac{1}{u^+ [(1/Pr - 1) + dy^+/du^+]} \frac{\partial^2 \theta}{\partial \xi^2}, \quad (25)$$

with the boundary conditions

$$\left. \begin{aligned} \theta &= 0 & \text{for all } u^+ & \text{and } \xi & \text{at } x^+ &= 0 \\ \theta &= 0 & \text{for } u^+ &= \infty & \text{and } \xi &= \infty & \text{at all } x^+ > 0 \\ \theta &= 1 & \text{for } u^+ &= 0 & \text{and } \xi &= 0 & \text{at all } x^+ > 0. \end{aligned} \right\} \quad (25a)$$

The introduction of the transformation (23) has reduced the working equation for  $Pr \neq 1$  to

a form identical with that for  $Pr = 1$ , except for the form of the function  $f(u^+)$  in (22) which must now be changed to

$$f[u^+(\xi)] = u^+ \left\{ \frac{1}{Pr} + 0.04432 \left[ e^{0.4u^+} - 1 - 0.4u^+ - \frac{1}{2}(0.4u^+)^2 + \frac{1}{6}(0.4u^+)^3 \right] \right\}. \quad (25b)$$

Just as before, interest is centred on the function

$$\begin{aligned} Sp(x^+, Pr) &= - \left( \frac{\partial \theta}{\partial u^+} \right)_{u^+=0} \\ &= - \left( \frac{\partial \theta}{\partial \xi} \right)_{\xi=0} \cdot Pr_e(0) \end{aligned}$$

so that

$$Sp(x^+, Pr) = - \left( \frac{\partial \theta}{\partial \xi} \right)_{\xi=0} \cdot Pr. \quad (26)$$

Calculations have been performed for  $Pr = 0.71, 7, 30, 100, 1000$  in addition to the value  $Pr = 1$  in [1]. The procedures were exactly the same as those followed in that reference, including the use of the solution for  $Pr \rightarrow \infty$

from [14, 15] to start the calculation with  $x^+ = 10$ .

The solution from equation (4) of [15] provides the function

$$\theta(y^+, x^+) = 1 - \frac{\gamma(1/3, \eta)}{\Gamma(1/3)} \quad (27)$$

where

$$\eta = \frac{(y^+)^3 Pr}{9x^+} \quad (27a)$$

and it is necessary in it first to transform from  $y^+$  to  $u^+$  with the aid of (9) and then to  $\xi$  with the aid of (24) which was integrated numerically by the Adams-Bashford method, i.e. by the scheme

$$\begin{aligned} \xi(u_n^+ + \Delta u^+) &= \xi(u_n^+) + \frac{\Delta u^+}{24} [9 Pr_e(u_n^+ + \Delta u^+) \\ &\quad + 19 Pr_e(u_n^+) - 5 Pr_e(u_n^+ - \Delta u^+) \\ &\quad + Pr_e(u_n^+ - 2\Delta u^+)] \quad (28) \end{aligned}$$

starting with  $\xi = 0$  at  $u^+ = 0$ .

The grid for the finite difference scheme is shown in Fig. 2. It differs from that in [1] merely

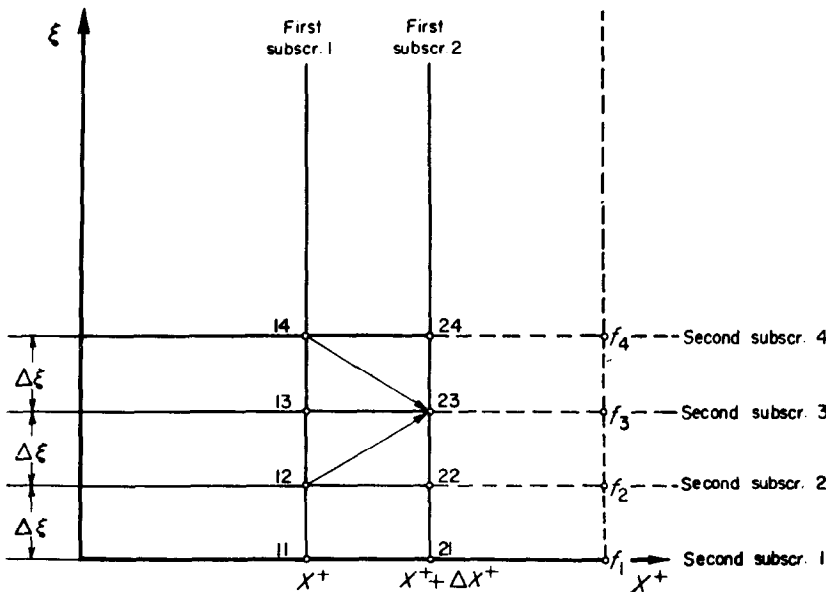
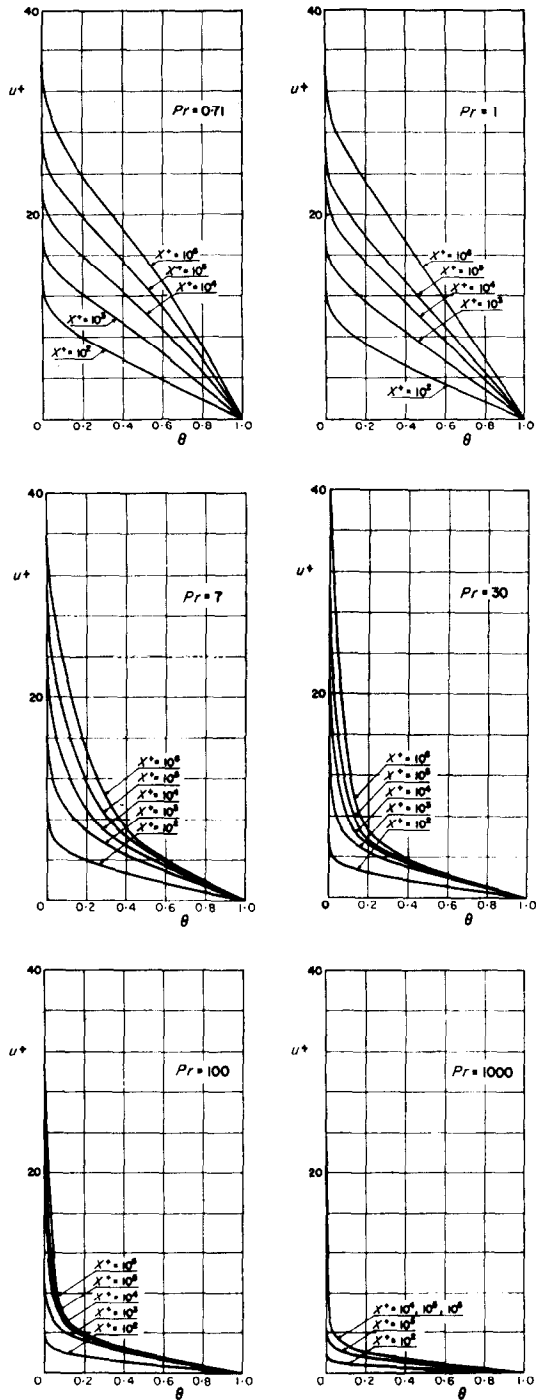


FIG. 2. Grid for the finite difference scheme.

Table 1. Steps required to preserve stability

Interval $x^+$	$\Delta x^+$	$\Delta \xi$	largest $\varphi$
<i>Pr = 0.71</i>			
10 to $10^2$	0.04	0.4	0.16
$10^2$ to $10^3$	0.08	0.4	0.32
$10^3$ to $10^4$	0.5	0.8	0.25
$10^4$ to $10^5$	4.0	1.6	0.33
$10^5$ to $10^6$	20.0	3.2	0.31
<i>Pr = 7</i>			
10 to $10^2$	0.05	1.6	0.30
$10^2$ to $10^4$	0.5	3.2	0.38
$10^4$ to $10^5$	4.0	6.4	0.37
$10^5$ to $10^6$	40.0	12.8	0.43
<i>Pr = 30</i>			
10 to $10^2$	0.05	4.0	0.36
$10^2$ to $10^4$	0.40	8.0	0.35
$10^4$ to $10^5$	4.0	16.0; 8.0	0.44
$10^5$ to $10^6$	25.0	32.0; 16.0	0.33
<i>Pr = 100</i>			
10 to $10^2$	0.025	7.0	0.37
$10^2$ to $10^3$	0.2	14.0; 7.0	0.36
$10^3$ to $10^4$	1.5	28.0; 7.0	0.44
$10^4$ to $10^5$	15.0	56.0; 7.0	0.42
$10^5$ to $10^6$	25.0	112.0; 7.0	0.30
<i>Pr = 1000</i>			
10 to $10^2$	0.04	40.0; 10.0	0.31
$10^2$ to $10^3$	0.4	80.0; 10.0	0.39
$10^3$ to $10^4$	1.6	160 ; 10.0	0.40
$10^4$ to $10^5$	10.0	320 ; 10.0	0.35
$10^5$ to $10^6$	20.0	320 ; 10.0	0.47



by the fact that the variable of integration is now  $\xi$  instead of  $u^+$ . The difference equation is

$$\theta(x^+ + \Delta x^+, \xi) = \theta(x^+, \xi) + \varphi[\theta(x^+, \xi + \Delta \xi) + \theta(x^+, \xi - \Delta \xi) - 2\theta(x^+, \xi)], \quad (29)$$

where

$$\varphi = \frac{\Delta x^+}{\bar{f}(\xi)(\Delta \xi)^2} \quad (29a)$$

The difference equation (29) permits us to calculate the temperature profile at  $x^+ + \Delta x^+$  in terms of  $\xi$  from the profile supposed to be known at  $x^+$ , that at  $x^+ = 10$  being given by

FIG. 3. Temperature profiles  $\theta(u^+, x^+)$  for  $x^+ = 10^2, 10^3, 10^4, 10^5, 10^6$  and for  $Pr = 0.71, 1, 7, 30, 100, 1000$ .

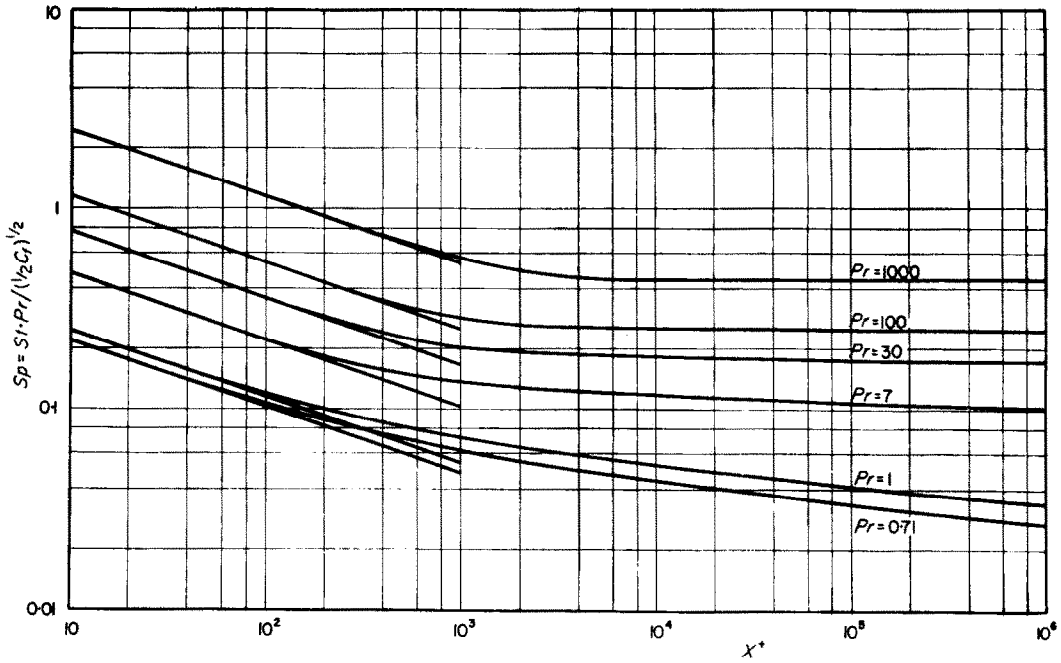


FIG. 4. The Spalding function  $Sp(x^+, Pr)$  in terms of  $x^+$  with  $Pr$  as parameter.

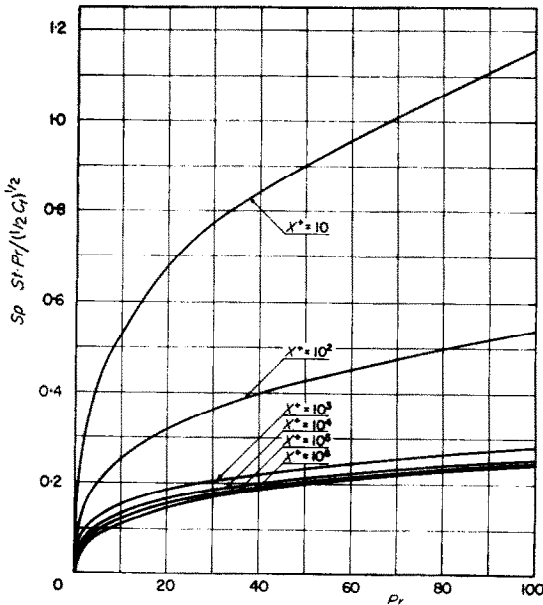


FIG. 5. The Spalding function  $Sp(x^+, Pr)$  in terms of  $Pr$  with  $x^+$  as parameter,  $Pr < 100$ .

(27) with the variables suitably changed. Thus, in Fig. 2,

$$\theta_{23} = \theta_{13} + \varphi_3(\theta_{12} + \theta_{14} - 2\theta_{13}) \quad (29b)$$

as in [1], except for the transformation of the independent variable from  $u^+$  to  $\xi$ .

The stability condition is still

$$\varphi = \frac{\Delta x^+}{f(\xi)(\Delta \xi)^2} < 0.5,$$

and in order to satisfy it the steps listed in Table I were chosen. In this connection it was found convenient to select larger steps  $\Delta \xi$  near  $\xi = 0$  and to decrease them as  $\xi \rightarrow \infty$  for Prandtl number values from 30 upwards. Consequently, the table lists the largest and smallest steps in  $\Delta \xi$  with the single largest value for  $\varphi$ .

It is recalled that the differential equation (25) is singular at  $\xi = 0$ . However, it can once again be shown that the curvature of the temperature

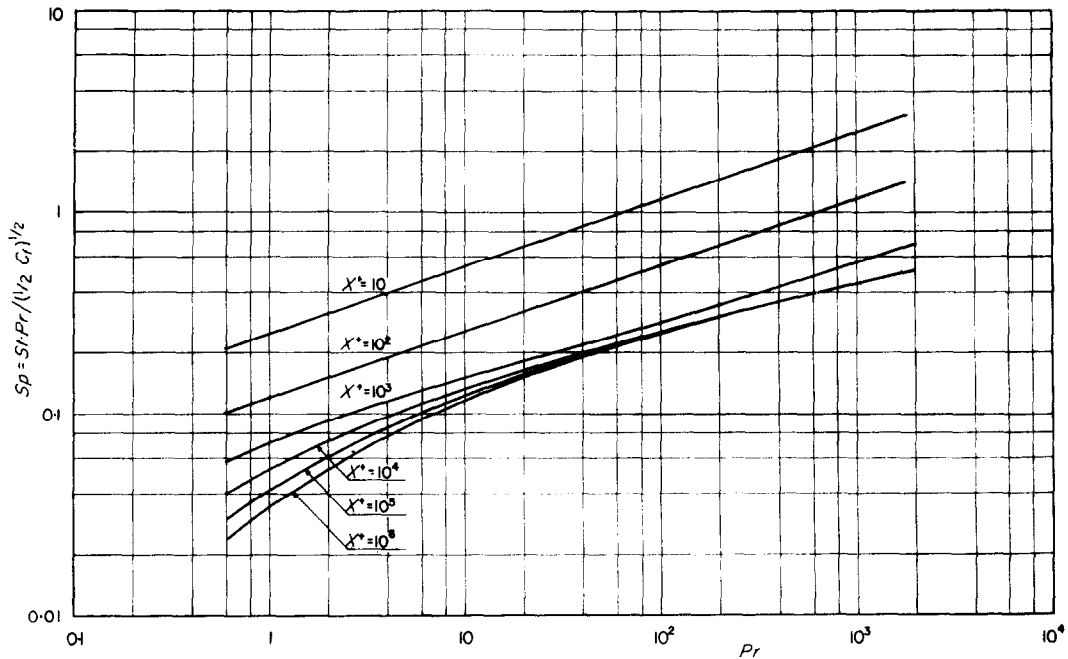


FIG. 6. The Spalding function  $Sp(x^+, Pr)$  in terms of  $Pr$  with  $x^+$  as parameter in a logarithmic plot.

profile  $\theta(\xi, x^+) = 0$  at  $\xi = 0$ , and to the present degree of approximation we can put

$$\theta_{22} = \frac{1 + \theta_{23}}{2} \quad (30)$$

instead of attempting to calculate  $\theta_{22}$  with the aid of (29b).

### 5. RESULTS OF CALCULATIONS

The results of the preceding calculations have been presented in a set of tables and diagrams, those for  $Pr = 1$  having been included for completeness.

The temperature profiles, plotted in terms of  $u^+$ , are given in Fig. 3. The values of the Spalding function, (21), i.e.

$$Sp(x^+, Pr) = \frac{St \cdot Pr}{(\frac{1}{2}C_f)^{1/2}} \quad (31)$$

are seen plotted in Figs. 4, 5 and 6. Fig. 4 shows a plot in terms of  $x^+$  with the Prandtl number as a parameter, Fig. 5 shows a plot in terms of Prandtl number for  $Pr < 100$ , and Fig. 6 shows the same plot for the full range of Prandtl numbers, but in logarithmic co-ordinates. The

diagram in Fig. 4 also shows the slopes

$$Sp(x^+, Pr) = \frac{0.53835}{(x^+)^{1/3}} Pr^{1/3} \quad (32)$$

which correspond to the asymptotic solution for  $Pr \rightarrow \infty$ . The Spalding function for various values of the Prandtl number has also been given in numerical terms in Table 2.

As might have been expected, and as seen from Figs. 5 and 6, the effect of varying the Prandtl number becomes progressively smaller as the Prandtl number is increased so that the large steps in Prandtl number from  $Pr = 30$  onwards do not impede interpolation.

The numerical relation between the intermediate variable  $\xi$  defined in (24) and the reduced velocity  $u^+ = u/v_*$  which has been obtained in the course of the present calculation can be utilized in a so-called Couette-type analysis. Accordingly, Table 3 lists values of the function  $u^+(\xi, Pr)$  with the Prandtl number as a parameter. Evidently, for  $Pr = 1$   $u^+ = \xi$  and the tabulation becomes superfluous. Unfortunately, in the course of the calculation it was not practicable to impose rounded-off values for either  $u^+$  or  $\xi$ .



Table 2. The Spalding function  $Sp(x^+, Pr)$ 

$x^+$	$Sp(x^+, Pr)$ for $Pr =$					
	0.71	1.0	7.0	30	100	1000
10	0.2228	0.2498	0.4779	0.7763	1.1598	2.4984
20	0.1771	0.1987	0.3793	0.6158	0.9203	1.9807
30	0.1554	0.1742	0.3321	0.5387	0.8047	1.7317
40	0.1418	0.1589	0.3023	0.4901	0.7317	1.5742
50	0.1322	0.1481	0.2813	0.4555	0.6798	1.4620
60	0.1249	0.1399	0.2653	0.4292	0.6402	1.3764
70	0.1191	0.1335	0.2525	0.4082	0.6086	1.3080
80	0.1144	0.1282	0.2421	0.3910	0.5826	1.2515
90	0.1105	0.1238	0.2334	0.3765	0.5606	1.2038
$1 \times 10^2$	0.1072	0.1200	0.2259	0.3640	0.5418	1.1628
2	0.08857	0.09929	0.1844	0.2934	0.4343	0.9260
3	0.08013	0.09012	0.1665	0.2614	0.3841	0.8135
4	0.07503	0.08466	0.1564	0.2427	0.3538	0.7435
5	0.07150	0.08092	0.1499	0.2303	0.3332	0.6946
6	0.06887	0.07815	0.1455	0.2217	0.3183	0.6581
7	0.06680	0.07598	0.1423	0.2154	0.3071	0.6295
8	0.06511	0.07423	0.1398	0.2107	0.2984	0.6064
9	0.06369	0.07276	0.1379	0.2071	0.2915	0.5874
$1 \times 10^3$	0.06248	0.07151	0.1363	0.2042	0.2859	0.5714
2	0.05555	0.06443	0.1288	0.1922	0.2628	0.4910
3	0.05220	0.06101	0.1258	0.1887	0.2575	0.4638
4	0.05007	0.05883	0.1240	0.1873	0.2557	0.4527
5	0.04853	0.05725	0.1227	0.1866	0.2550	0.4478
6	0.04734	0.05603	0.1217	0.1862	0.2545	0.4455
7	0.04638	0.05504	0.1209	0.1859	0.2542	0.4444
8	0.04557	0.05421	0.1202	0.1856	0.2540	0.4438
9	0.04488	0.05350	0.1196	0.1853	0.2537	0.4434
$1 \times 10^4$	0.04428	0.05288	0.1191	0.1851	0.2535	0.4431
2	0.04064	0.04908	0.1152	0.1828	0.2521	0.4420
3	0.03878	0.04712	0.1129	0.1812	0.2513	0.4418
4	0.03756	0.04581	0.1113	0.1800	0.2509	0.4418
5	0.03665	0.04484	0.1102	0.1792	0.2506	0.4418
6	0.03594	0.04407	0.1093	0.1786	0.2504	0.4417
7	0.03536	0.04345	0.1087	0.1781	0.2502	0.4417
8	0.03487	0.04291	0.1082	0.1778	0.2501	0.4417
9	0.03444	0.04245	0.1078	0.1776	0.2500	0.4417
$1 \times 10^5$	0.03407	0.04205	0.1705	0.1774	0.2499	0.4416
2	0.03168	0.03943	0.1060	0.1694	0.2490	0.4414
3	0.03047	0.03810	0.1052	0.1692	0.2484	0.4412
4	0.02966	0.03720	0.1044	0.1691	0.2479	0.4411
5	0.02905	0.03652	0.1037	0.1689	0.2475	0.4410
6	0.02857	0.03598	0.1031	0.1688	0.2472	0.4409
7	0.02817	0.03553	0.1025	0.1687	0.2469	0.4408
8	0.02784	0.03516	0.1019	0.1685	0.2467	0.4407
9	0.02756	0.03484	0.1013	0.1684	0.2466	0.4407
$10^6$	0.02731	0.03456	0.1008	0.1683	0.2464	0.4407

Table 3. Values of the function  $u^+$  ( $\xi, Pr$ ) for various values of the Prandtl number (Note that for  $Pr = 1$  we have  $u^+ = \xi$ )

$Pr = 0.71$		$Pr = 7.0$		$Pr = 30$		$Pr = 100$		$Pr = 1000$	
$u^+$	$\xi$	$u^+$	$\xi$	$u^+$	$\xi$	$u^+$	$\xi$	$u^+$	$\xi$
0.5650	0.4011	0.2290	1.603	0.1340	4.020	0.1400	14.00	0.0800	80.0
1.125	0.7988	0.4570	3.199	0.2660	7.980	0.2800	28.00	0.1600	160.0
1.690	1.200	0.6860	4.802	0.4000	12.00	0.4200	42.00	0.2400	240.0
2.255	1.601	0.9140	6.398	0.5340	16.02	0.5600	55.99	0.3200	320.0
2.815	1.999	1.143	8.000	0.6660	19.98	0.7000	69.98	0.4000	399.9
3.380	2.401	1.372	9.602	0.8000	24.00	0.8400	83.96	0.4800	479.8
3.940	2.800	1.601	11.20	0.9340	28.01	0.9800	97.91	0.5600	559.5
4.500	3.200	1.830	12.80	1.068	32.03	1.122	112.0	0.6420	641.0
5.055	3.598	2.060	14.40	1.200	35.98	1.264	126.1	0.7220	720.1
5.610	3.999	2.290	16.00	1.334	39.98	1.406	140.0	0.8040	800.7
6.160	4.400	2.521	17.60	1.468	43.98	1.550	154.1	0.8860	880.6
6.700	4.799	2.754	19.20	1.604	48.02	1.694	168.0	0.9680	959.7
7.235	5.199	2.988	20.80	1.738	51.99	1.842	182.0	1.052	1039.0
7.760	5.600	3.224	22.40	1.874	56.01	1.992	196.0	1.138	1119.0
8.275	6.001	3.464	24.00	2.010	59.99	2.146	209.9	1.226	1199.0
8.775	6.399	3.707	25.60	2.148	64.01	2.226	217.0	1.318	1280.0
9.265	6.798	3.955	27.20	2.286	67.99	2.306	224.0	1.412	1360.0
9.745	7.198	4.209	28.80	2.426	71.99	2.388	231.0	1.512	1440.0
10.22	7.599	4.471	30.40	2.714	80.02	2.472	238.0	1.618	1520.0
10.68	7.999	4.743	32.00	2.860	83.99	2.558	245.0	1.732	1600.0
11.13	8.398	5.027	33.60	3.012	88.02	2.648	252.1	1.794	1640.0
12.01	9.198	5.327	35.20	3.166	91.99	2.738	258.9	1.858	1680.0
12.87	10.00	5.647	36.80	3.326	95.99	2.834	266.0	1.926	1720.0
13.71	10.80	5.993	38.40	3.492	99.98	2.932	272.9	2.000	1760.0
14.54	11.60	6.373	40.00	3.666	104.0	3.036	280.0	2.078	1800.0
15.40	12.40	6.799	41.60	3.850	108.0	3.146	287.0	2.164	1840.0
16.17	13.20	7.284	43.20	4.046	112.0	3.260	294.0	2.258	1880.0
16.98	14.00	7.851	44.80	4.256	116.0	3.384	301.0	2.364	1920.0
17.79	14.80	8.527	46.40	4.486	120.0	3.516	308.0	2.484	1960.0
18.60	15.60	9.344	48.00	4.742	124.0	3.660	315.0	2.622	2000.0
19.40	16.40	10.33	49.60	5.032	128.0	3.818	322.0	2.790	2040.0
20.20	17.20	11.50	51.20	5.370	132.0	3.994	329.0	2.998	2080.0
21.01	18.00	12.83	52.80	5.778	136.0	4.194	336.0	3.276	2120.0
22.21	19.20	14.27	54.40	6.298	140.0	4.426	343.0	3.686	2160.0
23.01	20.00	15.79	56.00	7.006	144.0	4.706	350.0	3.826	2170.0
24.21	21.20	17.35	57.60	8.066	148.0	5.054	357.0	3.990	2180.0
25.41	22.40	18.92	59.20	9.834	152.0	5.514	364.0	4.186	2190.0
26.21	23.20	20.51	60.80	12.71	156.0	6.186	371.0	4.430	2200.0
27.41	24.40	22.11	62.40	16.39	160.0	7.334	378.0	4.746	2210.0
28.61	25.60	23.71	64.00	20.34	164.0	9.918	385.0	5.186	2220.0
29.81	26.80	25.30	65.60	24.33	168.0	15.53	392.0	5.878	2230.0
31.01	28.00	26.90	67.20	28.33	172.0	22.43	399.0	7.252	2240.0
32.21	29.20	28.50	68.80	32.33	176.0	29.43	406.0	11.65	2250.0
33.41	30.40	30.10	70.40	36.33	180.0	36.43	413.0	21.18	2260.0
34.61	31.60	33.30	73.60	40.33	184.0	43.43	420.0	31.18	2270.0
35.81	32.80	36.50	76.80	44.33	188.0	50.45	427.0	41.18	2280.0

## ACKNOWLEDGEMENTS

The authors wish to express their thanks to Prof. D. B. Spalding for his continued interest in the calculations and for several stimulating exchanges of letters. They also wish to thank Prof. W. Prager, Director of the Brown University Computing Center for his interest in the problem, and to the Administration of Brown University for financing the numerical calculations. Mr. B. C. Shen, Research Assistant at Brown University helped to check the calculations and to trace the diagrams. One of us (J. Kestin) was, in addition, partly supported by the research program of heat transfer in unsteady flows of the Aeronautical Research Laboratories, Office of Aerospace Research of the U.S. Air Force whose support is gratefully acknowledged.

## REFERENCES

1. J. KESTIN and L. N. PERSEN, Application of Schmidt's method to the calculation of Spalding's function and of the skin-friction coefficient in turbulent flow, *Int. J. Heat Mass Transfer*, **5**, 143-152 (1962).
2. A. G. SMITH and V. L. SHAH, The calculation of wall and fluid temperatures for the incompressible turbulent layer, with arbitrary distribution of wall heat flux, *Int. J. Heat Mass Transfer*, **5**, 1179 (1962).
3. D. B. SPALDING, Heat transfer to a turbulent stream from a surface with stepwise discontinuity in wall temperature, *Int. Dev. Heat Transfer*, Part II, p. 439, *ASME* (1961).
4. J. KESTIN and P. D. RICHARDSON, Heat transfer across turbulent, incompressible boundary layers. Proceeding of the Colloque International sur la Mécanique de la Turbulence, Marseilles (1961).
5. J. KESTIN and P. D. RICHARDSON, Heat transfer across turbulent incompressible boundary layers, *Int. J. Heat Mass Transfer*, **6**, 147, (1963).
6. O. REYNOLDS, On the extent and action of the heating surface for steam boilers, *Proc. Lit. Phil. Soc. Manchester*, **14**, 7-12 (1874).
7. D. COLES, *The Law of the Wall in Turbulent Shear Flow*. 50 Jahre Grenzschicht Forschung (Ed. by H. Görstler and W. Tollmien), p. 153-163. Vieweg, Braunschweig (1955).
8. D. COLES, The law of the wake in turbulent boundary layer, *J. Fluid Mech.* **1**, 191-226 (1956).
9. F. SCHULTZ-GRUNOW, Neues Widerstandsgesetz für glatte Platten, *Luftfahrtforsch.* **17**, 8 (1940): English translation, *NACA TM 986* (1951).
10. D. B. SPALDING, A single formula for the law of the wall, *J. Appl. Mech. Trans. ASME* **81**, Ser. E. No. 3, 455 (September 1961).
11. R. G. DESSLER, Analysis of turbulent heat transfer, mass transfer and friction in smooth tubes at high Prandtl and Schmidt numbers. *NACA TN 3145* (1954): also Report 1210 (1955).
12. P. S. KLEBANOFF, Characteristics of turbulence in a boundary layer with zero pressure gradient. *NACA TN 3178* (1954): also Report 1247 (1955).
13. E. SCHMIDT, Translation of *Thermodynamics* (1949), by J. Kestin, p. 428. Clarendon Press. Original papers, E. Schmidt, Föppl Festschr., Berlin (1927), and *Forschung* **13**, 177 (1942).
14. J. KESTIN and L. N. PERSEN, The transfer of heat across a turbulent boundary layer at very high Prandtl numbers, *Int. J. Heat Mass Transfer*, **5**, 355-371 (1962).
15. M. J. LIGHTHILL, Contribution to the theory of heat transfer through a laminar boundary layer, *Proc. Roy. Soc. A* **202**, 359 (1950).

**Résumé**—Cet article présente une tabulation importante de la fonction de Spalding  $Sp = St \cdot Pr / (\frac{1}{2} c_f)^{1/2}$  très utile dans le calcul des taux de transmission de chaleur dans les couches limites turbulentes. Les données numériques sont présentées pour  $Pr = 0,71, 1, 7, 30, 100$  et  $1000$ .

**Zusammenfassung**—Es werden ausführliche Tabellen der Spaldingfunktion  $Sp = St \cdot Pr / (\frac{1}{2} c_f)^{1/2}$  gebracht. Sie erweisen sich sehr nützlich bei der Berechnung des Wärmeüberganges in voll ausgebildeter turbulenter Grenzschicht. Die numerischen Angaben erstrecken sich auf  $Pr = 0,71; 1; 7; 30; 100$  und  $1000$ .

**Аннотация**—В статье приводятся подробные таблицы функции Сполдинга  $Sp = St \cdot Pr / (\frac{1}{2} c_f)^{1/2}$ , применяемые при расчете интенсивности переноса тепла в полностью развитом пограничном слое. Численные данные представлены для  $Pr = 0,71; 1,7, 30, 100$  и  $1000$ .